

A Practical Sense Amplifier Design for Memristive Crossbar Circuits (PUF)

Mesbah Uddin, and Garrett S. Rose

31st International System-on-Chip Conference (SOCC), Arlington, VA, USA, September 2018.

©2018 IEEE. Personal use of this material is permitted. Permission from IEEE must be obtained for all other uses, in any current or future media, including reprinting/republishing this material for advertising or promotional purposes, creating new collective works, for resale or redistribution to servers or lists, or reuse of any copyrighted component of this work in other works.

The online home for this paper may be found at: <http://web.eecs.utk.edu/~grose4/>

Citation Information (BibTex):

```
@INPROCEEDINGS{ISVLSI:Uddin2016,  
  author="M. Uddin and G. S. Rose",  
  title="A Practical Sense Amplifier Design for Memristive  
  Crossbar Circuits (PUF)",  
  booktitle="IEEE International System-on-Chip Conference  
  (SOCC) "  
  month="September",  
  year="2018",  
  pages="209-214",  
  address="Arlington, VA, USA"  
}
```

A Practical Sense Amplifier Design for Memristive Crossbar Circuits (PUF)

Mesbah Uddin and Garrett S. Rose

Department of Electrical Engineering and Computer Science

University of Tennessee, Knoxville

Knoxville, Tennessee 37996-2250

Email: {muddin6, garose}@utk.edu

Abstract—As CMOS process scaling is nearing to an end, emerging non-volatile devices such as memristors have been explored extensively in circuit design due to their very low footprint, non-volatility and low power application. Memristors, however, display a wide variety of characteristics depending on their inter-lying materials, as is the case for any emerging nano-devices. In this paper, we have designed a sense amplifier which is well-suited to applications of HfO_x memristor based crossbar circuits. Specifically, we have successfully integrated this sense amplifier into our memristive crossbar physical unclonable function (PUF) as a part of our chip that we are fabricating. Our designed sense amplifier is able to operate reliably and reasonably fast at near-to-ground input and low supply voltage and with small voltage differences between the bit-lines. We have performed several Monte Carlo analysis to choose optimal design and device parameters and thus evaluated our proposed design for real hardware applications.

I. INTRODUCTION

Memristors [1] have gained increased attention for the past few years because of their non-volatility, low switching energy, very low area and non-linear current-voltage characteristics. Here, we use the term ‘memristor’ to mean any of the metal-oxide semiconductors, transition metal-oxide, RRAM or ReRAM (resistive random access memory). Among the different memristor materials, HfO_x based memristors [2] are being explored by many groups due to their CMOS compatibility and very thin oxide layer implementation, among other advantages. Memristors can achieve a very high integration density within a crossbar architecture and thus memristive crossbars are being explored for memory and PUF circuits. In this work, we have designed and tuned our sense amplifier for a memristive crossbar PUF, the XbarPUF [3]. Specifically, we have designed a sense amplifier using 65nm CMOS process that is capable of operating with near-ground input voltages with small differences and with low supply voltage.

One of the major components in a dense memory architecture is the sense amplifier. The function of a sense amplifier is to sense voltage difference between two bit-lines of a memory and produce a full-swing rail-to-rail output during a memory read operation. For example, the sense amplifier can be used to determine a 1-bit response of the XbarPUF in place of an arbiter [4], [5]. A sense amplifier takes two column load voltages as its input bit-lines and determines which one is higher. Due to process variations in their respective memristive states and other parameters, memristors in two crossbar

columns have slightly different memristance and thus have slightly different voltage drop at the series load resistance. The sense amplifier attached at the bottom of each pair of XbarPUF columns detects small differences in load voltages to produce a digital PUF response.

For this work, we have experimented with several sense amplifier designs. First, we have narrowed down topology choices based on our design requirements. Then we have analyzed the selected ones in terms of reliability, performance, and energy overhead. We have looked in the literature for a sense amplifier topology which best suits our design requirements and is compatible for integration with memristive circuits. Then we have modified that topology to work properly for our circuits. We have run several Monte Carlo analysis by varying transistor lengths, widths and supply voltage to find best circuit parameters in terms of speed, energy consumption and yield or reliability and determine the applicability of our proposed design in a real hardware.

The contributions of this work include: (1) identifying the design constraints of a sense amplifier for HfO_x memristor and its crossbar based PUF architecture and thus development of the proposed sense amplifier; (2) comparison of the proposed design with other conventional sense amplifier designs; (3) evaluation of the proposed design in real hardware by running Monte Carlo analysis; (4) improvement of the design parameters from Monte Carlo analysis; (5) trade-off analysis of different design choices using delay, power and chip yield.

The paper is organized as follows: section II surveys and shortly describes different sense amplifier design topologies that might be useful for memristive crossbar circuits. Section III explains the design requirements for this particular sense amplifier design for HfO_x memristor based crossbar PUFs. Section IV presents and discusses our proposed sense amplifier design in details. Section V presents the experimental results and provides the analyses and rationale for our work. Finally, future prospects and concluding remarks are provided in section VI and VII, respectively.

II. BACKGROUND

Various types of sense amplifier (SA) topologies and designs have been considered for this work. We have built each type of SA circuit and analyzed them to evaluate their strengths and weaknesses with respect to our application. There are

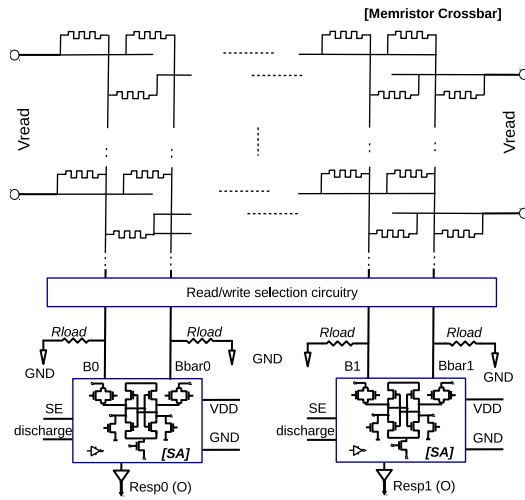


Fig. 2. Application of the proposed sense amplifier for a memristive crossbar PUF (XbarPUF [4])

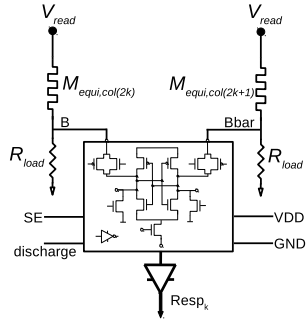


Fig. 3. An equivalent input-output circuit for our proposed sense amplifier in XbarPUF [4]

line voltages near to GND rail and with small voltage differences between those bit-lines. Available supply voltage and frequency choices are also limited. As we'll show later, VLSA works faster at low supply voltage and near-to-ground bit-lines than other sense-amplifier topologies, these requirements imply an SA design based on VLSA. The impact of threshold voltage (V_t) mismatch and beta-mismatch (β) are also low in VLSA than CLSA [6], [13] and that impact can be reduced further more reliably by increasing the transistor width in VLSA compared to CLSA. Lower mismatch means higher bit-line resolution and considering both the design requirements, we have chosen VLSA topology for our sense amplifier design. The schematic of our proposed sense amplifier design is shown in Fig. 1.

The input bit-line voltages are applied at diffusions of access transistors, M5-M8, in Fig. 1 and thus the SA circuit offers low input resistances to these bit-lines. The inputs are taken from the voltage division node between equivalent crossbar memristors and the series load resistance and, therefore, do not have infinite drive strength. If VDD is used, at the top of the design in Fig. 1 instead of 'SE' signal, VDD can affect through the PMOS transistors and affect/change the sampled voltage at nodes 'O' and 'Ob' during input sampling phase. Therefore, the most important modification compared

to traditional VLSA has been done to detach the supply while sampling bit-line voltages into these internal nodes. The supply voltage of sensing PMOS transistors are tied to the sense enable signal, 'SE' in Fig. 1. Thus, when the SA is in sampling state, 'SE' remains low to ensure no current path is formed as well as voltage from the source of PMOS transistors do not interfere and change the latched voltage. During sensing, the signal 'SE' would provide power for the resolving of the two nodes 'O' and 'Ob'. Fig. 2 shows this application of our proposed SA design for the XbarPUF [5] when our SA is used to determine which crossbar column has higher voltage drop across its load resistor. Fig. 3 shows the input-output equivalent circuit for the SA during the response generation or 'read' operation of the XbarPUF. All memristors of a crossbar column form a resistor division circuit with the load resistor. The voltage from adjacent column load resistors are used as the two inputs to the sense amplifier as shown in Fig. 3. The sense amplifier compares and then produces a '1' or '0', full swing output. Additional buffers may also be used.

At low supply voltage, the time needed for latching of inputs to internal nodes of this type of SA become large and thus can dominate the overall performance. Unlike traditional VLSA, instead of using just NMOS or PMOS for access transistors, we have used both as transmission gates which increase the input voltage range of operation by passing analog input voltages reliably to internal nodes. Since our input voltages are near to GND, the NMOS transistors in the transmission gates are made stronger compared to PMOS ones.

Two additional NMOS transistors M10 and M11 are used to discharge the two internal sensing nodes 'O' and 'Ob', in Fig. 1. They discharge these nodes to zero or ground so that they do not add any bias to the next sensing operation. However, these two transistors are optional and can be omitted if at the end of sensing, two zero-input voltage are latched into these internal nodes, thereby resetting them. Moreover, for our XbarPUF application, response is generated only once during power-up and, therefore, there is no need for next sensing operation and thus we may totally omit this zeroing state. For other memristor crossbar architecture like an RRAM (memory), either these two transistors or a zeroing phase would be useful.

As a base, all transistor lengths are chosen to be at minimum length of $L_{unit} = 60nm$. Transistor widths are sized as follows: the four access transistors, M5-M8 in Fig. 1 are sized $W_{unit} = 1.2\mu m$ each, top two PMOS transistors, M1-M2 are also sized $1.2\mu m$ while M3-M4 are sized $2 * W_{unit} = 2.4\mu m$. With equal sizes, NMOS access transistors are actually stronger than PMOS access transistors which is desirable since the two bit-line voltages to be sampled are closer to ground than to VDD. Their sizes are also chosen to be large enough to have negligible drop across them. M1-M4 transistors forms two equal sized cross-coupled inverters where NMOS are made stronger. The two discharge transistors, M10 and M11 are sized with $2.4\mu m$ to have a fast recharge phase as well as quick discharge of both nodes (close to ground). The lone inverter, in Fig. 1 and if any additional buffers used are sized properly to comply with the input and output load demands

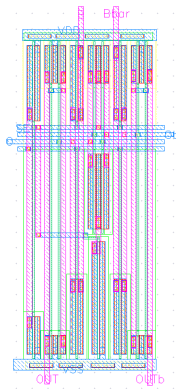


Fig. 4. Layout of the proposed sense amplifier done using 65nm technology (Dim: $10.9\mu\text{m} \times 4.2\mu\text{m}$)

and are usually a few times larger than minimum. All these sizes might be scaled up to reduce mismatch and improve yield as we have shown later.

There are three states of operation for this sense amplifier based crossbar PUF or memory design. During the READ phase, sense enable signal, ‘SE’ of Fig. 1 is kept low. This is the input voltage sampling state where voltage across column load resistors are sampled into sense amp’s internal nodes ‘O’ and ‘Ob’. During the next sensing phase, signal ‘SE’ is enabled high and thus supply is enabled and bottom NMOS transistor is turned on as well to ensure a path from VDD (high SE) to GND. The node with higher voltage resolves to VDD while the other node resolves to GND. The signal, ‘SE’ should be kept high during this whole time which provides the power for the sensing operation. In last or third phase, both internal nodes ‘O’ and ‘Ob’ are discharged to ground to make the sense amplifier ready for next sensing operation. A small spike of around 50ns pulse is applied at the gates of discharge transistors for this purpose. Equal-sized buffers or buffer-chains can be used to separate the internal output nodes, ‘O’ and ‘Ob’ from outside and to be able to drive larger load. Buffers add zero or negligible delay due to relatively slower rising or falling nature of internal output nodes during sensing phase compared to the rise/fall time of inverters in buffers.

Fig. 4 shows the layout for this proposed SA plus two output buffers. Since this is for the XbarPUF, discharge transistors are not used in this particular layout. The layout of the SA is made symmetric for the cross-coupled inverters to remove any bias to any input bit-lines. Internal connections and wire lengths and widths are designed such a way that both ‘O’ and ‘Ob’ nodes have the same output load. One important thing is that the SA layout is intentionally made taller rather than a wide multi-finger design for the sake of crossbar circuits. Because an SA is needed for each pair of columns of an XbarPUF as shown in Fig. 2, wide SAs would eventually increase the overall pitch of the memristor crossbar and thus each SA should be as narrow as possible without degrading performance. This design is being fabricated now and there is also a guard ring around each SA on the chip to mitigate noise from other circuit components. As analyzed in [13], finger

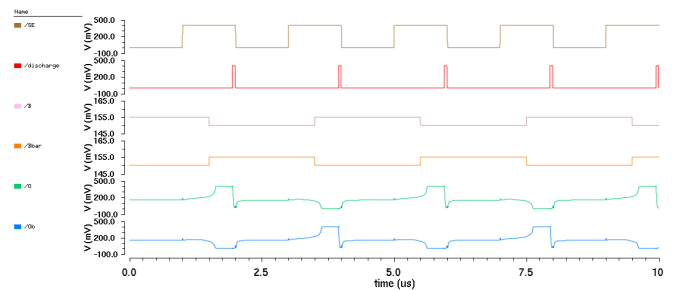


Fig. 5. Waveforms for transient simulation of proposed SA for input bit-line voltages of 150mV and 155mV with VDD = 0.4V

numbers or sizes do not affect VLSA-based designs and thus our choice of finger widths is only to keep low aspect ratio and minimize area and comply with the pitch of the attached memristor crossbar.

TABLE I
COMPARISONS AMONG DIFFERENT SA TOPOLOGIES

Topology	Conventional (CLSA) [7]	VLSA [14]	PCSA [11]	Proposed
Precharge needed	yes/no	yes	no	no
Avg. delay (μs)	2.75	3.51	0.62	0.27
Avg. power ($n\text{W}$)	0.48	0.77	0.42	0.63 / 0.19

V. RESULTS, ANALYSES AND DISCUSSION

As mentioned in last section, fast operation under low supply voltage with low input bit-line voltages, high resolution of bit-line voltage difference, and compatibility with memristor crossbar architectures are the driving forces behind choosing our particular SA design. We have built and experimented with different SA circuit topologies and compared against our design. Table I lists the comparison among different SA designs where the supply or VDD is kept at 0.4V and bit-line voltages are 150mV and 155mV. For fair comparison, for each of the design, same unit length (60nm) and width ($1.2\mu\text{m}$) are used to generate the data for this table. It can be seen that our proposed design is by far the fastest among them. Both the CLSA [7] and VLSA [14] work very slowly at this bit-line voltage range. The PCSA (pre-charge SA) from [11] consumes smaller power with relatively high speed. Our proposed design has comparatively high power consumption when discharge transistors are used. However, without those two, our proposed design has also the lowest power consumption among these designs. The power consumption of Table I includes dynamic power of inverter and power consumption during all phases of the SA. Another thing to note is that because of the high delay of some of these designs, the results of Table I are generated using a lower frequency with clock period of $12\mu\text{s}$ instead of the required maximum of $2\mu\text{s}$. Therefore, actual power consumption would be higher.

Fig. 5 displays the waveforms for our implemented SA design at 0.4V VDD with bit-line voltages of 150mV and 155mV (‘B’ and ‘Bbar’ in Fig. 1). The clock or sense enable signal ‘SE’ has a period of $2\mu\text{s}$. The value of the input signals

TABLE II
PERCENT YIELD OF PROPOSED SENSE AMPLIFIER FOR DIFFERENT
TRANSISTOR SIZES AND SUPPLY VOLTAGE

Transistor sizes	$(\frac{W}{L})$	$(\frac{W}{3L})$	$(\frac{3W}{3L})$	$(\frac{2W}{5L})$	$(\frac{5W}{5L})$
VDD = 0.4V	67.35	72.45	78.55	83.25	87.20
VDD = 0.6V	64.20	77.20	89.70	90.70	98.50
VDD = 0.9V	61.10	73.10	84.70	87.00	95.50
VDD = 1.2V	60.50	72.70	84.30	87.20	95.40

‘B’ and ‘Bbar’ are flipped on each clock cycle to see if our design can resolve to opposite values quickly. A discharge signal of $50ns$ duty cycle with same $2\mu s$ time period is used to discharge the output nodes ‘O’ and ‘Ob’ at the end of each sensing phase. During sensing (‘SE’ goes high), ‘O’ and ‘Ob’ resolves either VDD or GND, based on which of the ‘B’ or ‘Bbar’ signal is high. The output is valid before discharge signal is high and a sufficient delay after ‘SE’ goes high. Outputs should be alternating on each cycle with ‘O’ and ‘Ob’ of resolving to opposite values and that is what it can be seen in Fig. 5.

We have run Monte Carlo analysis to determine the reliability of the proposed design. For each Monte Carlo run, we have applied two input pairs, one where output should be a ‘1’ and one where output is a ‘0’. The clock period is chosen to be $2\mu s$ with 50% duty cycle, suitable for the XbarPUF. Thus $1\mu s$ is being allotted for sensing phase plus a $50ns$ discharge phase. The input voltages are 150mV and 155mV initially, flipped on the second cycle to get both a ‘1’ and ‘0’ output on consecutive cycles. The supply voltage and widths and lengths of the transistors are varied for different runs. To determine the best circuit parameters i.e. length and width of each transistor and the supply voltage, we have run Monte Carlo analysis for 500 chips for our proposed design with different (W/L) ratios and different supply voltages. Here in the table, $W = W_{unit} = 1.2\mu m$ and $L = L_{unit} = 60nm$ (min. length of this 65nm technology). As expected, increasing the length and (W/L) ratio increase transistor area and thus reduce mismatch, thereby improves the yield of the design considerably. It can also be seen from Table II that with increasing VDD, yield decreases. It can be explained by the fact that input voltages are close to GND and, therefore, with higher VDD, there is a higher magnitude of leakage which corrupts output nodes at the start of sensing and just after latching of input to those nodes, thereby reducing yield. However, with a sub-threshold VDD (at 0.4V VDD where for this technology, V_{th} is around 500-550mV), the delay is longer while clock frequency is unchanged and, therefore, it may not resolve for all cases due to additional delay arising from mismatch. Thus, at 0.4V, our design has the lowest yield compared to above-threshold supply voltages as in many instances the SA doesn’t get enough time to give a full-swing output. Although for the leftmost column of transistors with unit length (60nm), yield is actually highest for 0.4V VDD. The reason is that SA operates very fast with transistor length being very small and thus decreasing effect of additional mismatch delay is less

TABLE III
SENSING DELAY (ns) OF PROPOSED SENSE AMPLIFIER FOR DIFFERENT
TRANSISTOR SIZES AND SUPPLY VOLTAGE

Transistor sizes	$(\frac{3W}{3L})$	$(\frac{2W}{5L})$	$(\frac{5W}{5L})$
VDD = 0.4V	712	625	627
VDD = 0.6V	19.63	16.7	16.7
VDD = 0.9V	1.02	1.524	1.523

TABLE IV
ENERGY(JOULE) PER CYCLE OF PROPOSED SENSE AMPLIFIER FOR
DIFFERENT TRANSISTOR SIZES AND SUPPLY VOLTAGE

Transistor sizes	$(\frac{3W}{3L})$	$(\frac{2W}{5L})$	$(\frac{5W}{5L})$
VDD = 0.4V	20.66f	16.79f	41.79f
VDD = 0.6V	0.80p	0.50p	1.26p
VDD = 0.9V	11.08p	5.54p	13.65p

than the yield improvement achieved by lowering VDD. From Table II, it can be concluded that for overall better yield ($\geq 80-85\%$), larger transistor sizes (rightmost three columns of Table II) should be considered.

Larger transistor sizes reduce mismatch and thus improve yield, but they also contribute to larger area, delay and energy overhead. Therefore, there is a trade-off between yield and delay plus energy overhead of the circuit. To find delay and energy consumption, we have experimented with the transistor sizes listed in Table II, except for the (W/L) and (W/3L) as their yield are too low and thus are not considered for further analysis. A VDD of 1.2V is not also considered as it increases the power consumption considerably. Table III lists the sensing delay for the selected three transistor sizes with relative better yield where Table IV lists the total energy consumption during one cycle of the designed SA. From these two tables, it can be found that transistor size of (2W/5L) i.e. $240\mu m$ width and $300nm$ length gives a much lower sensing delay as well as low conversion energy at 0.6V VDD, compared to other. Its area and leakage should also be lower compared to the other two sizes as width and (W/L) ratio are smaller. However, depending on the design requirements and application, a trade-off among yield, delay, energy consumption and total area can be easily made from these analysis.

VI. FUTURE WORK

We have implemented our sense amplifier in a chip designed with 65nm process. After fabrication, we can get the actual characteristics from this circuit implementation. An XbarPUF which uses a few of these sense amplifiers is also being fabricated. Therefore, the next step after getting that chip back is to measure SA performance in a real application on a fabricated chip. We can also measure and analyze performance change due to mismatch from manufacturing variations or variations due to temperature, aging, supply rail noise or any other environmental factors from the implementation.

VII. CONCLUSION

The whole schematic and layout design has been done using Cadence Virtuoso with 65nm technology. Even though

65nm process can be considered small for analog design, we choose 65nm process for this design as well to comply with other circuit components of our whole work there. As this sense amplifier is designed primarily for memristor based crossbar circuits, new design constraints are imposed compared to any traditional CMOS analog circuits. The layout is drawn manually and is symmetric to both the inputs and outputs and therefore, our proposed design actually is shown to resolve very small input voltage differences pretty fast. The validity and effectiveness of our proposed design in a practical application is validated by several different Monte Carlo runs. These Monte Carlo runs help to gather insights about the circuit parameters to choose them more wisely.

ACKNOWLEDGMENT

The authors would like to thank Dr. Md. Sakib Hasan, Aysha S. Shanta, and Md. Badruddoja Majumder of our research group for interesting discussions related to this topic.

This material is based upon work supported by the Air Force Office of Scientific Research under award number FA9550-16-1-0301. Any opinions, finding, and conclusions or recommendations expressed in this material are those of the authors and do not necessarily reflect the views of the United States Air Force.

REFERENCES

- [1] D. B. Strukov, G. S. Snider, D. R. Stewart, and R. S. Williams, "The missing memristor found," *Nature*, vol. 453, pp. 80–83, May 2008.
- [2] K. Beckmann, H. Manem, and N. Cady, "Performance enhancement of a time-delay PUF design by utilizing integrated nanoscale ReRAM devices," *IEEE Trans. on Emerging Topics in Computing*, p. 1, 2016.
- [3] G. Rose and C. Meade, "Performance analysis of a memristive crossbar PUF design," in *52nd ACM/EDAC/IEEE Design Automation Conference (DAC)*, June 2015, pp. 1–6.
- [4] M. Uddin, M. B. Majumder, G. S. Rose, K. Beckmann, H. Manem, Z. Alamgir, and N. C. Cady, "Techniques for improved reliability in memristive crossbar PUF circuits," in *IEEE Comp. Society Annual Symp. on VLSI (ISVLSI)*, July 2016, pp. 212–217.
- [5] M. Uddin, M. B. Majumder, K. Beckmann, H. Manem, Z. Alamgir, N. C. Cady, and G. S. Rose, "Design considerations for memristive crossbar physical unclonable functions," *J. Emerg. Technol. Comput. Syst.*, vol. 14, no. 1, pp. 2:1–2:23, sep 2017.
- [6] B. Mohammad, P. Dadabhoy, K. Lin, and P. Bassett, "Comparative study of current mode and voltage mode sense amplifier used for 28nm SRAM," in *24th Int. Conf. on Microelectronics (ICM)*. IEEE, 2012, pp. 1–6.
- [7] T. Kobayashi, K. Nogami, T. Shirotori, and Y. Fujimoto, "A current-controlled latch sense amplifier and a static power-saving input buffer for low-power architecture," *IEEE J. of Solid-State Circuits*, vol. 28, no. 4, pp. 523–527, Apr 1993.
- [8] M. R. Garg and A. Tonk, "A study of different types of voltage & current sense amplifiers used in SRAM," *Int. J. of Advanced Research in Computer and Communication Engineering*, vol. 4, May 2015.
- [9] A. Lee, C.-C. Lin, T.-C. Yang, and M.-F. Chang, "An embedded ReRAM using a small-offset sense amplifier for low-voltage operations," in *VLSI Design, Automation and Test (VLSI-DAT), 2015 Int. Symp. on*. IEEE, 2015, pp. 1–4.
- [10] M. F. Chang, C. W. Wu, C. C. Kuo, S. J. Shen, K. F. Lin, S. M. Yang, Y. C. King, C. J. Lin, and Y. D. Chih, "A 0.5v 4mb logic-process compatible embedded resistive RAM (ReRAM) in 65nm CMOS using low-voltage current-mode sensing scheme with 45ns random read time," in *IEEE International Solid-State Circuits Conference*, Feb 2012, pp. 434–436.
- [11] W. Zhao, C. Chappert, V. Javerliac, and J. P. Noziere, "High speed, high stability and low power sensing amplifier for MTJ/CMOS hybrid logic circuits," *IEEE Trans. on Magnetics*, vol. 45, no. 10, pp. 3784–3787, Oct 2009.
- [12] D. Zhang, L. Zeng, T. Gao, F. Gong, X. Qin, W. Kang, Y. Zhang, Y. Zhang, J. O. Klein, and W. Zhao, "Reliability-enhanced separated pre-charge sensing amplifier for hybrid CMOS/MTJ logic circuits," *IEEE Transactions on Magnetics*, vol. 53, no. 9, pp. 1–5, Sept 2017.
- [13] J. Yeung and H. Mahmoodi, "Robust sense amplifier design under random dopant fluctuations in nano-scale CMOS technologies," in *IEEE Int. SOC Conf.*, Sept 2006, pp. 261–264.
- [14] D. Rennie and M. Sachdev, "SRAM sense amplifier," Sep. 17 2013, uS Patent 8,536,898. [Online]. Available: <https://www.google.com/patents/US8536898>